

# Joint Route Selection and Radio Resources Allocation for Caching in Multi-Hop Networks

Emre Gures, *Graduate Student Member, IEEE*, Pavel Mach, *Member, IEEE*, and Zdenek Becvar, *Senior Member, IEEE*,

**Abstract**—In this paper, we focus on a cache-enabled networks, where a content requested by user equipments (UEs) can be delivered by means of multi-hop relaying via unmanned aerial vehicles (UAVs) and/or via other UEs exploiting device-to-device (D2D) communication. For such scenario, we optimize transmission power allocation, bandwidth allocation, and route selection to minimize the content delivery duration. The formulated problem is a mixed-integer nonlinear programming (MINLP) problem and, thus, it is hard to solve. Hence, we first solve the power and bandwidth allocation by a cooperative game among all transmitting nodes involved in the content delivery process and we prove that this game is a potential game. Then, we introduce a fast-converging iterative algorithm employing an approximate better-response mechanism for the resource allocation (i.e., power and bandwidth). After that, we design a low-complexity greedy algorithm jointly handling route selection and power and bandwidth allocation. The algorithm selects transmission routes to deliver the requested contents to the UEs and, after each selection, the resource allocation at the transmitting nodes involved in the content delivery process (i.e., GBS, UAVs, and relaying UEs) is updated. The simulation results demonstrate that the proposed scheme reduces the average content delivery duration by up to 23.2% compared to the best-performing benchmark algorithm.

**Index Terms**—caching, content delivery duration, D2D, UAV, multi-hop relaying, resource allocation, game theory.

## I. INTRODUCTION

The advent of the sixth generation (6G) mobile networks is poised to meet the unprecedented data transmission demands generated by a multitude of communicating devices, including smartphones, sensors, vehicles, or various internet of things (IoT) devices. This surge in connectivity is expected to place significant demands on high data rate and low-latency communication in mobile networks. By caching frequently requested content close to the end users, such as at ground base stations (GBSs), data transmission across the core network can be avoided resulting in reduced latency and energy consumption of the network [1].

Furthermore, the use of unmanned aerial vehicles (UAVs) as aerial caching nodes and/or relays can significantly enhance the performance of caching. The reason is that the UAVs can be rapidly deployed and positioned above areas with high user density or temporarily increased traffic demand (e.g., concerts, festivals, or sports events), providing additional capacity and improved coverage without the cost and rigidity of installing

new fixed base stations [2]. Moreover, by operating at higher altitudes than buildings, the UAVs are more likely to establish line-of-sight links to ground users and to other UAVs. As a result, the UAVs are particularly beneficial in urban scenarios with blockages and makes them effective relays in multi-hop content delivery. Similarly, the benefits of content caching can be amplified by using neighboring user equipments (UEs) as relay UEs (RUEs) to deliver the content through device-to-device (D2D) communication [3].

The combination of content caching at the GBSs and the UAVs along with relaying via the UAVs and/or the UEs represents a multi-faceted content delivery architecture suited for emerging 6G mobile networks. Still, there are many fundamental challenges to be addressed in order to fully unlock the potentials of caching via the the D2D and the UAVs, including power and bandwidth allocation, route selection, deployment of the UAVs, or selection of content provider. In this regard, number of works address power allocation along with content provider selection or route selection in cache-enabled UAV-assisted D2D cellular networks in order to minimize secrecy rate among requesting UEs [4], maximize the sum capacity [5], [6], maximize content hit ratio [7], or maximize energy efficiency [8], [9]. None of these works, however, targets minimization of the content delivery duration, which is one of the key parameters for caching from the UEs perspective.

The minimization of content delivery duration in the cache-enabled UAV and D2D-assisted networks is addressed in [10], where the authors optimize content placement, computational resource allocation, and UAV deployment. Further, in [11], the authors optimize content placement in order to minimize the content delivery duration. Besides, the authors in [12] optimize user association, content placement, and UAV deployment with the objective of minimizing the weighted sum of content delivery duration, energy consumption, and UAV deployment cost.

All aforementioned works, however, assume only a direct communication [7], [9], [10], [12] or, at most, to two-hop communication via a single UAV relay [4], [5], [6], [8], [11]. However, as the distance between the place where the content is cached and the requesting UE increases, or as the communication environment deteriorates due to obstacles or interference, the direct communication or even two-hop communication is generally insufficient to reduce the content delivery duration [13]. Note that deploying many conventional fixed GBSs can reduce content delivery duration, albeit at a significant installation cost. In this regard, the content delivery over multi-hop transmission that leverages on relaying of

E. Gures, P. Mach, and Z. Becvar are with the Faculty of Electrical Engineering, Czech Technical University in Prague, Prague, Czech Republic, Email: {guresemr, machp2, zdenek.becvar}@fel.cvut.cz

This work was supported by the project SGS26/005/OHK3/1T/13 funded by the Czech Technical University in Prague.

UAVs and RUEs is typically required to provide alternative transmission routes, thereby reducing the overall content delivery duration.

An extension of existing solutions to multi-hop scenarios is not straightforward due to the tight coupling among decision variables of the optimization problem. Besides, conventional multi-hop routing protocols, such as the optimized link state routing (OLSR) or the ad hoc on-demand distance vector (AODV) are not directly suitable for the considered cache-enabled multi-hop network since both: *i*) operate at the network layer and construct routes based on simple link metrics, like hop count, *ii*) assume fixed link capacities and ignore joint transmission power and bandwidth allocation, and *iii*) are not cache-aware, since the source and destination of each flow are determined outside the routing protocol.

Furthermore, all closely related works focusing on caching in UAV and D2D communication scenarios (i.e., [4]-[12]) do not exploit efficient radio resource management. First of all, all works (i.e., [4]-[12]) adopt fixed bandwidth allocation. Moreover, among the works considering up to two-hop communication, the works [5], [6], [8] simplify the optimization problem by fixing the capacity of the GBS-UAV link, while the works [4], [11] determine the capacity of this link based on fixed GBS transmission power. Besides, majority of works focusing on caching in scenario with UAVs and D2D communication assume that transmitting nodes (i.e., GBS, UAVs, and RUEs) send contents sequentially, i.e., each content is transmitted one after another while maximum transmission power is allocated to each content [4], [5], [6], [8], [9], [10], [11]. Hence, the existing works are not able to efficiently minimize delivery duration of individual contents as the content delivery duration is strongly dependent on the allocated bandwidth and transmission power. At the same time, the sequential transmission of contents inevitably prolongs the average transmission duration, since the delivery of each content is deferred until the delivery of the previous content is completed.

Another major limitation of most of the works addressing multiple key challenges is that these works first decompose the optimization problem into sub-problems and, then, solve these sub-problems separately rather than through joint optimization of all variables [4], [5], [6], [8], [9], [10], [12]. However, the joint optimization of multiple sub-problems is essential to minimize the content delivery duration, since individual sub-problems, such as transmission route selection, transmission power, and bandwidth allocation, are tightly coupled with each other in multi-hop networks. This coupling arises because the transmission route selection depends on the relationship between requesting UEs and nodes, while the resource allocation affects this relationship, creating strong interdependency among route selection, transmission power, and bandwidth allocation. Unlike iterative methods that handle sub-problems separately, joint optimization simultaneously considers all decision variables across the network, directly capturing their strong interdependencies and ensuring coordinated and consistent decisions. Although a joint solution is provided in [7], the authors address different problems (i.e., power allocation and content provider selection) and different objective (i.e., maximizing content hit ratio) with respect to our work.

In view of the conducted research explained above, the joint optimization of route selection, transmission power allocation, and bandwidth allocation in cache-enabled multi-hop network with goal to minimize content delivery duration has not yet been addressed in the literature. Thus far, joint optimization of transmission power and bandwidth allocation has not been addressed even in simple direct or two-hop communication scenarios. Also, no work considers simultaneous transmission of multiple contents by each node (GBS, UAV, or RUE). The joint consideration of multi-hop communication and simultaneous transmission of contents in our work introduces strong interdependencies among optimization variables inevitably altering the required solution compared not only to the direct communication scenarios, but also to the existing works considering two-hop communication.

Our main contributions are summarized as follows:

- We formulate an optimization problem for route selection, power allocation, and bandwidth allocation in cache-enabled multi-hop networks to minimize the sum content delivery duration. In this regard, we propose an optimization framework jointly handling route selection, power allocation, and bandwidth allocation, accounting for interdependencies among the optimized variables.
- We propose dynamic transmission power and bandwidth allocation at each transmitting node (i.e., GBS, UAV, or RUE) and to all contents currently being sent. To this end, we first formulate the joint power and bandwidth allocation problem as a cooperative resource allocation game among all transmitting nodes and prove that this game is a potential game. Building on this formulation, we propose an iterative algorithm using an approximate better-response mechanism for resource allocation to minimize the sum content delivery duration.
- We propose a low-complexity greedy algorithm jointly optimizing route selection and resource allocation. Specifically, after the route for any content is selected, the resource allocation (i.e., transmission power and bandwidth) at the nodes involved in the content delivery process is updated. The updated allocation reflects its impact on the delivery durations of other contents whose delivery routes have not yet been selected. Therefore, the proposed algorithm explicitly captures the interdependencies between route selection and resource allocation decisions, enabling resource allocation updates that directly account for their mutual impact on the overall content delivery duration.
- We demonstrate that our proposed framework reduces an average content delivery duration by up to 23.2% compared to the best-performing state-of-the-art algorithm.

This paper extends our prior conference works [15], [16]. The paper [15] addresses route selection and power allocation in the multi-hop cache-enabled networks. Then, [16] further optimizes power allocation by simple heuristic solution. This paper, then, significantly extends [15], [16], towards joint optimization of route selection, transmission power allocation, and bandwidth allocation adopting game theory-based framework.

The rest of this paper is organized as follows. Section

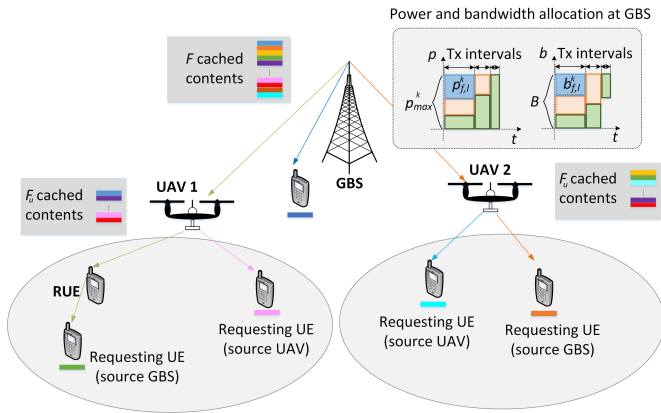


Fig. 1: A cache enabled multi-hop network in urban area.

II introduces the system model. Section III formulates the targeted problem. The proposed resource allocation algorithm is explained in Section IV. In Section V, we present the proposed joint route selection and resource allocation algorithm. Section VI discusses the implementation aspects of the proposed framework. Simulation results are presented in Section VII while Section VIII concludes this paper.

## II. SYSTEM MODEL

This section describes the network model, the cache placement model, content delivery options and model of the content delivery duration.

### A. Network Model

We consider a cache-enabled multi-hop network with the UAVs and D2D communication, as depicted in Fig. 1. The system includes  $N$  UEs, where  $M$  UEs request a specific content for delivery, while the remaining  $N - M$  UEs not currently requesting any content can act as the RUEs to facilitate more efficient content dissemination via D2D relaying [3]. The content can be delivered from  $1 + U$  base stations, including one GBS and  $U$  UAVs acting as aerial relay stations. As in [17], the UAVs are assumed to be deployed at fixed positions during content delivery. This assumption reflects practical deployment scenarios, such as concerts, festivals, or sports events, where the UAVs hover at fixed locations and serve dense user populations in a confined area without significant impact on coverage quality [18], [19]. Consequently, balloon- or airship-based UAVs are seen suitable, since they consume negligible propulsion energy while static and are repositioned only if the performance of the served UEs falls below specific requirements, as shown in [20].

### B. Cache Placement Model

We assume that there are  $F$  available contents from which each UE can request one content. The size of any  $f$ -th content is denoted as  $S_f$ . The UEs request contents according to a given content popularity distribution  $\gamma = \{\gamma_1, \gamma_2, \dots, \gamma_F\}$ , where  $\gamma_f$  is the request probability for the  $f$ -th content and, thus,  $\sum_f \gamma_f = 1$ . We model the content popularity with

commonly used Zipf distribution [21]. Hence, the popularity of the  $f$ -th content is calculated as:

$$\gamma_f = \frac{f^{-\lambda}}{\sum_{j=1}^F j^{-\lambda}} \quad (1)$$

where  $\lambda$  is the Zipf exponent indicating the degree of skewness in the popularity, with  $0 < \lambda \leq 1$  [22]. More specifically, large  $\lambda$  implies a more concentrated distribution of requests for certain contents while smaller  $\lambda$  implies that the content request probability is distributed more evenly.

The GBS serves as the central repository for all available contents. Besides, the UAVs may also cache the contents. Since the UAVs have limited storage capacity, they can store only a subset of these contents, denoted as  $F_u$ . To manage content storage, we employ a probabilistic cache placement strategy [23], [24], where each UAV independently decides whether to cache the  $f$ -th content with probability  $\gamma_f$ . This decision is made independently for each UAV, i.e., even if all UAVs have the same storage capacity, they may cache different contents.

### C. Content Delivery Options

Depending on content placement, each content can be delivered to the requesting UEs by one of the following options: *i*) directly by the GBS from its central repository, *ii*) directly by one of the UAVs if the UAV caches the content requested by the UE, or *iii*) by relaying the content via the UAVs and/or the RUEs. In case of the last option, we employ half-duplex operation for the UAVs and RUEs, as full-duplex transmission, although theoretically advantageous for reducing content delivery duration, suffers from self-interference and interference from simultaneous transmissions on the same resources [25]. The selection of a particular delivery route is indicated by the binary variable  $x_{m,f,r} \in \{0, 1\}$ , where  $x_{m,f,r} = 1$  if the  $m$ -th requesting UE asks for the  $f$ -th content to be delivered via the  $r$ -th route, and  $x_{m,f,r} = 0$  otherwise.

### D. Content Delivery Duration

We assume that the area is served by single GBS, which has bandwidth  $B$  at its disposal. Then, the GBS assigns a dedicated and non-overlapping channels for transmission of contents to each UE either directly or via multi-hop communication. Consequently, simultaneous transmissions from different nodes are spectrally isolated (i.e., separated in the frequency domain), ensuring that mutual interference among the GBS, UAVs, and RUEs does not occur within the area.

Furthermore, each transmitting node has  $p_{\max}^k$  transmission power allocation budget that is distributed among currently transmitted contents. Each  $f$ -th content may be transmitted by a given node over  $L$  multiple transmission (Tx) intervals, with potentially varying bandwidth and power allocations in each interval (see illustrative example in Fig. 1, where the GBS transmits three contents over three Tx intervals allocating different transmission power over varying bandwidth). Then, the portion of the  $f$ -th content transmitted during the  $l$ -th transmission interval by the  $k$ -th transmitting node (i.e., GBS, UAV or RUE) is further denoted as  $S_{f,l}^k$ . Accordingly, the

overall content delivery duration for the  $f$ -th content requested by the  $m$ -th UE whilst using the  $r$ -th transmission route is defined as follows:

$$t_{m,f,r} = \sum_l \frac{S_{f,l}^k}{b_{f,l}^k \log_2 \left( 1 + \frac{p_{f,l}^k \tilde{g}_{k,k'}}{b_{f,l}^k (\sigma_0 + I_b)} \right)} \quad (2)$$

where  $p_{f,l}^k$  and  $b_{f,l}^k$  is the transmission power and the bandwidth allocated by the  $k$ -th node to the transmission of the  $f$ -th content during the  $l$ -th interval, respectively,  $\sigma_0$  is the noise power,  $\tilde{g}_{k,k'}$  is the instantaneous channel gain between the  $k$ -th transmitting node and the  $k'$ -th receiving node, and  $I_b$  is the background interference emulating the aggregated inter-cell interference originating from neighboring cells outside the area covered by the GBS.

We assume a realistic wireless environment, where channel gain is affected by fading. Thus, in (2),  $\tilde{g}_{k,k'}$  is calculated as  $\tilde{g}_{k,k'} = g_{k,k'} |g_{k,k'}^f|^2$ , where  $g_{k,k'}$  is the large-scale channel gain (capturing path-loss and potential attenuation due to a building blockage) and  $g_{k,k'}^f$  represents the small-scale fading coefficient. In addition, we also incorporate uncertainties in the channel quality (e.g., due to a channel estimation or prediction error) between the  $k$ -th transmitting node and the  $k'$ -th receiving node ( $\Delta g_{k,k'}$ ). Thus, channel gain between any  $k$ -th and  $k'$ -th nodes is  $\hat{g}_{k,k'} = g_{k,k'} + \Delta g_{k,k'}$  [26], [27].

### III. PROBLEM FORMULATION

The objective of this paper is to minimize the sum content delivery duration for all contents requested by the UEs via jointly optimizing the route selection  $\mathbf{x}$ , transmission power allocation  $\mathbf{p}$ , and bandwidth allocation  $\mathbf{b}$  at the transmitting nodes. Thus, the optimization problem is formulated as:

$$\begin{aligned} & \min_{\mathbf{x}, \mathbf{p}, \mathbf{b}} \quad \sum_m \sum_f \sum_r x_{m,f,r} t_{m,f,r} \\ \text{s.t.} \quad & (3a) \quad \sum_r x_{m,f,r} \leq 1, \quad \forall m, f \\ & (3b) \quad \sum_f p_{f,l}^k = p_{\max}^k, \quad \forall l, k \\ & (3c) \quad 0 \leq p_{f,l}^k \leq p_{\max}^k, \quad \forall f, l, k \\ & (3d) \quad \sum_f b_{f,l}^k = B, \quad \forall l, k \\ & (3e) \quad 0 \leq b_{f,l}^k \leq B, \quad \forall f, l, k \\ & (3f) \quad \sum_l S_{f,l}^k = S_f, \quad \forall f \\ & (3g) \quad 0 \leq S_{f,l}^k \leq S_f, \quad \forall f, l \end{aligned} \quad (3)$$

where constraint (3a) ensures that each content is delivered through at most one transmission route, (3b) guarantees the total power allocated by the  $k$ -th transmission node to all currently transmitted contents does not exceeds its maximum power budget  $p_{\max}^k$  at any  $l$ -th transmission interval, (3c) ensures the power allocated to the  $f$ -th content during the  $l$ -th interval is non-negative and does not exceed the maximum power budget  $p_{\max}^k$ , (3d) guarantees that the sum of bandwidth allocated across all transmitting nodes and all contents at each  $l$ -th transmission interval does not exceed the total system bandwidth  $B$ , (3e) ensures the bandwidth allocated to the  $f$ -th content during the  $l$ -th interval is non-negative and does

not exceed system's total bandwidth  $B$ , (3f) ensures that the  $f$ -th content is fully delivered with all its parts by each  $k$ -th transmission node, and (3g) guarantees that the size of the  $k$ -th content transmitted during any  $l$ -th interval is non-negative and does not exceed the total size of content  $S_f$ .

The above-formulated problem is a mixed-integer nonlinear programming (MINLP) problem since the power and bandwidth allocation variables ( $p$  and  $b$ ) are continuous, whereas the route selection  $x$  is integer variable. Besides, the objective function in (3) is non-convex due to a coupling among all decision variables. Furthermore, the coupling between binary and continuous decision variables introduces nonlinearities in the constraints and contributes to the non-convexity of the solution space (see (2)). Such MINLP problems are NP-hard, hence, there is no known polynomial-time algorithm for solving such problems optimally [28]. Therefore, we first formulate the joint optimization of transmission power and bandwidth allocation at all transmitting nodes as a cooperative resource allocation game, prove that it is a potential game, and solve it via an iterative algorithm based on an approximate better-response mechanism (Section IV). Leveraging the proposed resource allocation framework, we then propose a greedy algorithm tailored to jointly manage route selection and resource allocation (Section V).

### IV. PROPOSED RESOURCE ALLOCATION

In this section, we provide a high-level overview of the proposed resource allocation (power and bandwidth allocation) principle, we describe the proposed solution based on game theory, and analyze upper bound on number of iterations.

#### A. High-level Description of Proposed Resource Allocation

The proposed resource allocation scheme dynamically allocates both transmission power and bandwidth among multiple simultaneously transmitted contents to minimize the content delivery duration for the requesting UEs. The main objective of the proposed resource allocation principle is to fully utilize the transmission power at each node and the entire bandwidth across all simultaneously transmitted contents, ensuring efficient use of network resources and minimizing the sum content delivery duration. Specifically, once the transmission of a particular content is completed, the resources previously allocated to that content are reallocated among the remaining active content transmissions, ensuring that the released resources are promptly utilized to accelerate the delivery of the remaining contents. Hence, the duration of each transmission interval depends on the transmission power and bandwidth allocations, content sizes, and channel conditions, all of which collectively impact the completion durations of the transmitted contents.

Building upon the network model presented in Fig. 1, Fig. 2 illustrates the proposed resource allocation principle through an example involving the concurrent transmission of five contents. Initially, the GBS allocates its entire transmission power and bandwidth across three different contents: *Content 1*, *Content 2*, and *Content 3*. Once the transmission of *Content 1* is completed, the power and bandwidth previously allocated to *Content 1* are released and immediately reallocated to *Content*

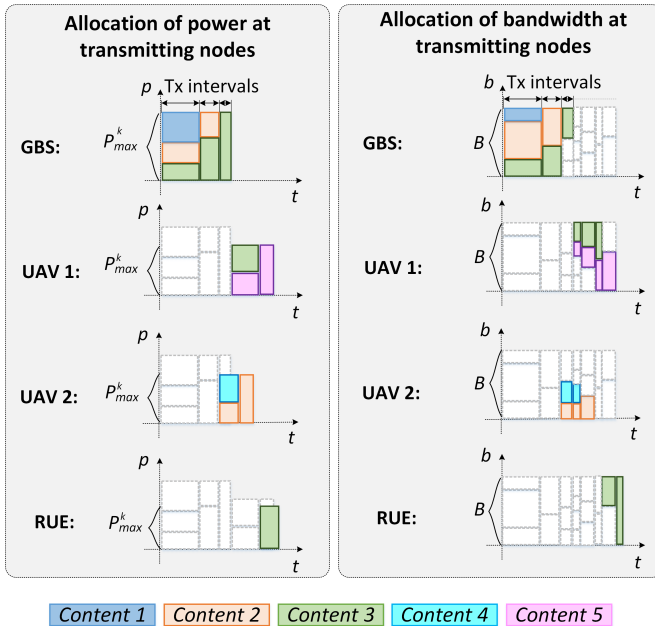


Fig. 2: The cached contents, distinguished by different colors, are requested by different UEs and delivered either directly by the GBS/UAVs or relayed via UAVs and/or RUEs through D2D communication. Transmission power and bandwidth allocated to each content in individual Tx intervals is also distinguished by colors.

2 and *Content 3*. Following the delivery of *Content 2* to the UAV2, the GBS updates its resource allocation accordingly. Thus far, the UAV2 operated in the reception mode due to half-duplex operation, receiving *Content 2* from the GBS while being unable to transmit any content. As a result, only the GBS reallocates its resources during first two intervals. After *Content 2* is fully received at the UAV 2, however, the UAV 2 switches from the reception to the transmission mode, enabling it to forward *Content 2* to the requesting UE while simultaneously initiating the transmission of *Content 4* that is stored directly at the UAV 2. Consequently, both the GBS and UAV 2 reallocate their transmission power and bandwidth across the ongoing content transmissions. Specifically, the GBS dedicates its entire transmission power and bandwidth to *Content 3*, while UAV 2 distributes its available resources between *Content 2* and *Content 4*. Similarly, once *Content 3* is fully transmitted by the GBS, UAV 1 switches to transmission mode, forwarding *Content 3* to the RUE while simultaneously initiating the transmission of *Content 5*. This process of resource reallocation continues until all contents are fully delivered.

The resource allocation decisions made at each transmission node affect not only the contents being transmitted at that node during the current and subsequent intervals, but also influence the resource allocation decisions at other nodes in subsequent intervals. For instance, allocating more power and bandwidth to *Content 1* at the GBS during interval 1 may reduce the delivery duration of *Content 1*, but at the cost of decreasing the resources available for *Content 2* and *Content*

3, potentially increasing the delivery duration of *Content 2* and *Content 3*. However, if the transmission of *Content 1* is completed earlier by allocating more resources to *Content 1* in interval 1, the power and the bandwidth previously allocated to *Content 1* are released sooner. Then, the released resources can be reallocated to accelerate the delivery of *Content 2* and *Content 3*. As a result, the overall delivery duration for *Content 2* and *Content 3* may ultimately be reduced, despite the initial prolongation of their delivery duration. Moreover, resource allocation at the GBS impacts the time when the UAV 1 and the UAV 2 switch to the transmission mode. This, in turn, influences the overall delivery duration of their respective contents (i.e., *Content 3* and *Content 5* for UAV 1, and *Content 2* and *Content 4* for UAV 2). This timing effect is particularly critical in multi-hop scenarios, where the interconnected nature of content delivery creates strong interdependencies in the resource allocation decisions across transmitting nodes. Due to this dynamic interplay in resource allocation, the distribution of transmission power and bandwidth is determined in advance, before any content is being transmitted.

In the next section, we describe in detail the proposed resource allocation algorithm.

### B. Proposed Resource Allocation Based on Game Theory

In this section, we describe our solution for joint transmission power allocation and the bandwidth allocation. To this end, we first formulate the sub-problem of transmission power allocation and the bandwidth allocation as follows:

$$\begin{aligned} \min_{p,b} \quad & \sum_m \sum_f \sum_r t_{m,f,r} \\ \text{s.t.} \quad & (3b), (3c), (3d), (3e), (3f), (3g) \end{aligned} \quad (4)$$

The resource allocation at individual transmitting nodes (i.e., GBS, UAVs, and RUEs) are temporally (across transmission intervals) and spatially (across nodes in the network) interdependent due to the multi-hop structure of the network. Since the resource allocation at one node affects both when and how other nodes can allocate their transmission power and bandwidth, a coordinated approach is essential. Therefore, we adopt a game theory approach to make the distributed decisions (including transmission power and bandwidth allocation) at individual transmitting nodes while considering coupling among their strategies. Game theory is particularly suitable for modeling the resource allocation problems [29], [30], as it captures the interactions among multiple transmitting nodes whose transmission power and bandwidth allocation decisions are interdependent due to simultaneous content transmissions and the multi-hop structure of the network.

To this end, we model the problem as a cooperative resource allocation game, defined by the triplet  $G = \{\mathcal{K}, \{s_k\}_{k \in \mathcal{K}}, \{U_k\}_{k \in \mathcal{K}}\}$ , where:

- **Players:**  $\mathcal{K}$ , denoted by  $\mathcal{K} = \{k_1, k_2, \dots, k_K\}$ , is a set of players including all the transmitting nodes involved in the content delivery process (i.e., the GBS, the UAVs, and the RUEs).

- **Strategy:** Each  $k$ -th player selects a resource allocation strategy  $s_k \in \mathcal{S}_k$ , where  $\mathcal{S}_k$  is the finite set of feasible resource allocation strategies for the  $k$ -th player. The resource allocation strategy  $s_k$  consists of the transmission power and bandwidth allocations  $\{p_{f,l}^k, b_{f,l}^k\}$  across all  $F$  contents and all  $L$  transmission intervals, such that:

$$s_k = \left\{ p_{f,l}^k, b_{f,l}^k \left| \begin{array}{l} \sum_f p_{f,l}^k = p_{\max}^k, \quad \sum_m \sum_f b_{f,l}^k = B, \\ p_{f,l}^k \geq 0, b_{f,l}^k = 0, \forall l \end{array} \right. \right\}$$

- **Utility:** The joint strategy profile of the game is  $s = (s_{k_1}, s_{k_2}, \dots, s_{k_K}) \in \mathcal{S}$ , where  $\mathcal{S} = \mathcal{S}_{k_1} \times \mathcal{S}_{k_2} \times \dots \times \mathcal{S}_{k_K}$  is the Cartesian product of all players' individual strategy spaces. Each  $k$ -th player has a utility function  $U_k(s)$ , which depends on both its own resource allocation strategy  $s_k$  and the resource allocation strategies of all other players, denoted by  $s_{-k}$ .

**Lemma 1.** *The cooperative resource allocation game is a potential game.*

*Proof.* A game is a potential game if there exists a potential function  $\Phi$  such that, for any player  $k \in \mathcal{K}$  and any two arbitrary strategies  $s'_k$  and  $s''_k \in \mathcal{S}_k$ , the following holds:

$$\Phi(s'_k, s_{-k}) - \Phi(s''_k, s_{-k}) = U_k(s'_k, s_{-k}) - U_k(s''_k, s_{-k}), \quad (5)$$

where  $\Phi(s'_k, s_{-k})$  and  $\Phi(s''_k, s_{-k})$  are the values of potential function of the game quantifying the overall network utility under two different joint strategy profiles if the  $k$ -th player adopts the strategy  $s'_k$  or  $s''_k$ , respectively, and all other players adopt the strategy profile  $s_{-k}$ ,  $U_k(s'_k, s_{-k})$  and  $U_k(s''_k, s_{-k})$  are the values of individual utility functions to measure the payoff of the  $k$ -th player, i.e., the effect of choosing  $s'_k$  or  $s''_k$  on the network performance when the strategies of the other players  $s_{-k}$  are fixed.

In the proposed game, all players cooperate to minimize the sum content delivery duration. However, since potential games are typically defined as maximization problems, each player's utility function is defined as the negative of the sum content delivery duration. Therefore, each player's utility function is defined identically as the network utility:

$$U_k(\mathbf{s}) = U_{\text{network}}(\mathbf{s}) = - \sum_m \sum_f \sum_r t_{m,f,r}(\mathbf{s}) \quad (6)$$

Since all players share the same utility function given by the network utility in (6), the condition in (5) is satisfied. Hence, the cooperative resource allocation game is a potential game with the potential function:

$$\Phi(\mathbf{s}) = U_k(\mathbf{s}) = U_{\text{network}}(\mathbf{s}), \forall k \quad (7)$$

Consequently, because all players have identical utilities, the game is classified as an identical-interest game, which is a strict case of potential games. ■

Identical-interest games inherit all theoretical properties of potential games; therefore, all theoretical properties of potential games are applicable, and the cooperative resource allocation game is subject to these properties [31], [32]. Specifically,

every finite potential game has at least one pure strategy Nash equilibrium, and all Nash equilibria are either local or global maximizers of the potential function [33]. Moreover, there are several learning mechanisms, such as better-response [34] and best-response [35], that are guaranteed to converge to a Nash equilibrium in potential games.

In the best-response mechanism, at each iteration, each player explores its entire strategy space and selects the resource allocation strategy that minimizes the network utility, assuming the strategies of all other players remain fixed. The best-response mechanism offers fast convergence, but requires significant computational complexity, as each player should search its entire strategy space. In contrast, under the better-response mechanism, each player randomly selects an alternative strategy at each iteration and updates its strategy only if the alternative strategy results in a higher network utility than the current one. The better-response mechanism reduces computational complexity by avoiding an exhaustive search over the entire strategy space, albeit at the cost of slower convergence compared to the best-response. Consequently, a trade-off exists between convergence speed and computational complexity when comparing these two mechanisms.

To solve the cooperative resource allocation problem, we adopt an iterative algorithm that allocates transmission power and bandwidth across multiple contents for each player, based on an approximate better-response mechanism, as detailed in Algorithm 1. This iterative algorithm incorporates randomness into the decision process, which enables convergence to the globally optimal solution with high probability [36], [37]. First, Algorithm 1 initializes the iteration index  $i = 0$  and sets  $\Delta$ , the gradient norm of the potential function, to  $\infty$ , ensuring that the algorithm continues to iterate until either convergence is achieved or the maximum number of iterations is reached (see line 1 in Algorithm 1). Then, an initial resource allocation  $s_k^0 \in \mathcal{S}_k$  is set for all players, where the total transmission power and bandwidth of each  $k$ -th player are equally distributed among the currently transmitted contents (line 2). This equal allocation serves as a neutral starting point that satisfies the feasibility constraints and ensures that no content is initially prioritized, allowing the algorithm to iteratively adjust the allocation to minimize the sum content delivery duration [37]. The joint strategy vector  $s^0 = (s_{k_1}^0, s_{k_2}^0, \dots, s_{k_K}^0)$  is then formed, and the initial potential function  $\Phi(s^0)$  is calculated, serving as initial reference utility for the game (line 3).

Algorithm 1 updates the resource allocation at each iteration and terminates when the norm of the gradient of the potential function  $\Delta$  falls below a predefined threshold  $\epsilon$ , or when the maximum number of iterations is reached (lines 4–18). At each iteration, all players  $k \in \mathcal{K}$  sequentially update their resource allocation strategies  $s_k \in \mathcal{S}_k$  using an approximate better-response mechanism, assuming the strategies of all other players  $s_{-k}$  remain fixed during their individual updates. Specifically, at the  $i$ -th iteration, each  $k$ -th player selects a new alternative strategy  $s_k^{\text{new}} \in \mathcal{S}_k$  (line 6). The player then computes the utility values  $U_k(s_k^{\text{new}}, s_{-k}^i)$  and  $U_k(s_k^i, s_{-k}^i)$  representing the network utility adopting the alternative strategy  $s_k^{\text{new}}$  and the current strategy  $s_k^i$ , respectively, while all other nodes retain their strategies  $s_{-k}^i$  (line 7). If the utility

---

**Algorithm 1** Iterative resource allocation algorithm
 

---

```

1:  $i \leftarrow 0, \Delta \leftarrow \infty$ 
2: Select an initial resource allocation  $s_k^0, \forall k \in \mathcal{K}$ 
3: Set  $s^0 \leftarrow (s_{k_1}^0, s_{k_2}^0, \dots, s_{k_K}^0)$  and compute  $\Phi(s^0)$ 
4: while  $\Delta \geq \epsilon$  and  $i < i_{\max}$  do
5:   for each player  $k \in \mathcal{K}$  do
6:     Select a new strategy  $s_k^{\text{new}} \in S_k$ 
7:     Compute  $U_k(s_k^{\text{new}}, s_{-k}^i)$  and  $U_k(s_k^i, s_{-k}^i)$ 
8:     if  $U_k(s_k^{\text{new}}, s_{-k}^i) < U_k(s_k^i, s_{-k}^i)$  then
9:       Set  $s_k^{i+1} \leftarrow s_k^{\text{new}}$ 
10:    else
11:      Set  $s_k^{i+1} \leftarrow s_k^i$ 
12:    end if
13:  end for
14:  Set  $s^{i+1} \leftarrow (s_{k_1}^{i+1}, s_{k_2}^{i+1}, \dots, s_{k_K}^{i+1})$ 
15:  Compute  $\Phi(s^{i+1})$ 
16:   $\Delta = \|\nabla\Phi(s^{i+1})\|_\infty$ 
17:   $i \leftarrow i + 1$ 
18: end while
    
```

---

value  $U_k(s_k^{\text{new}}, s_{-k}^i)$  is lower than  $U_k(s_k^i, s_{-k}^i)$ , the  $k$ -th player updates its strategy  $s_k^{i+1}$  at the iteration  $i + 1$  to  $s_k^{\text{new}}$  (i.e.,  $s_k^{i+1} = s_k^{\text{new}}$ ) (line 9); otherwise, the  $k$ -th player retains its current strategy (i.e.,  $s_k^{i+1} = s_k^i$ ) (line 11). After all players update their resource allocation strategies, the joint strategy profile is formed as  $s^{i+1} = (s_{k_1}^{i+1}, s_{k_2}^{i+1}, \dots, s_{k_K}^{i+1})$ , which serves as the input for the next iteration (line 14). The potential function  $\Phi(s^{i+1})$  corresponding to the updated joint strategy vector is then computed to evaluate the network utility at the iteration  $i + 1$ . Last, the change in the potential function is assessed as  $\Delta = \|\nabla\Phi(s^{i+1})\|_\infty$ , which quantifies the steepest rate of change in the network utility at the current iteration and is used to evaluate convergence toward a local optimum (line 16) and the iteration index is incremented by one, i.e.,  $i \leftarrow i + 1$  (line 17).

The computational complexity of Algorithm 1 is  $O\left(\sum_{l=1}^L F_l \cdot I\right)$ , where  $L$  is the total number of transmission intervals,  $F_l$  is the number of transmitted contents in the  $l$ -th interval, and  $I$  is the maximum number of iterations required for convergence during the  $l$ -th interval. At each iteration, the algorithm updates the transmission power and bandwidth allocations for all transmitted contents within the interval. The number of iterations  $I$  required at each transmission interval depends on the number of contents transmitted during that interval, the degree of interdependency in resource allocation among the nodes involved in content delivery, and the total number of transmission intervals. The total number of transmission intervals depends on both the number of requesting UEs and the hop counts of their delivery routes.

### C. Analysis of upper bound on number of iterations

This section analyses a theoretical upper bound on the number of iterations in Algorithm 1. Thus, we analyze the behavior of the potential function  $\Phi(s)$  along the iterate sequence  $\{s^i\}$ , where  $s^i$  denotes the joint resource-allocation profile at the

$i$ -th iteration. For the  $k$ -th node, under the approximate better-response update in Algorithm 1, the strategy update satisfies:

$$\Phi(s_k^{i+1}, s_{-k}^i) \geq \Phi(s_k^i, s_{-k}^i), \quad (8)$$

with strict inequality whenever the new resource-allocation strategy is adopted. Consequently,

$$\Phi(s^{i+1}) - \Phi(s^i) = \sum_{k \in \mathcal{K}} [\Phi(s_k^{i+1}, s_{-k}^i) - \Phi(s_k^i, s_{-k}^i)] \geq 0, \quad (9)$$

which implies that the potential function  $\Phi(s)$  is monotonically non-decreasing and upper-bounded. In order to obtain the upper bound on the number of iterations, we first relate the per-iteration improvement  $\Phi(s^{i+1}) - \Phi(s^i)$  to the stopping condition  $\|\nabla\Phi(s^i)\|_\infty < \epsilon$ . This is formally characterized by the following lemma, which holds when the potential function has a Lipschitz-continuous gradient on the feasible region.

**Lemma 2 (smoothness).** *Consider two consecutive iterates  $s^i$  and  $s^{i+1}$  that lie in the relative interior of the feasible set  $\mathcal{S}$ . For all indices  $(k, f, l)$  that contribute to the objective (i.e.,  $S_{f,l}^k > 0$ ), the corresponding allocations satisfy  $p_{f,l}^k > 0$  and  $b_{f,l}^k > 0$ . Then, the potential function  $\Phi(s)$  is twice continuously differentiable ( $C^2$ ) on any compact subset of this region and its gradient is Lipschitz continuous. Consequently, there exists a finite constant  $\alpha < \infty$  such that:*

$$\|\nabla\Phi(s^{i+1}) - \nabla\Phi(s^i)\|_2 \leq \alpha \|s^{i+1} - s^i\|_2, \quad (10)$$

*Proof.* Each term of  $\Phi(s)$  takes the form

$$t(p, b) = \frac{S}{b \log_2 \left(1 + \frac{pg}{b(\sigma_0 + I_b)}\right)}, \quad (11)$$

which is  $C^2$  in  $(p, b)$  over the region  $\{(p, b) : 0 < p \leq p_{\max}, 0 < b \leq B\}$ . Since  $\Phi(s)$  is a finite linear combination of such terms in  $(p, b)$ ,  $\Phi(s)$  is  $C^2$  wherever all bandwidth allocations used in these terms are strictly positive. On any compact subset of this region (with  $p$  bounded by  $p_{\max}^k$  and  $b$  bounded by  $B$ ), the Hessian  $\nabla^2\Phi(s)$  is continuous and, hence, bounded; therefore, there exists:

$$\alpha = \max_{s \in \mathcal{S}} \|\nabla^2\Phi(s)\|_2 < \infty, \quad (12)$$

which, by the mean-value argument, implies

$$\|\nabla\Phi(s^{i+1}) - \nabla\Phi(s^i)\|_2 \leq \alpha \|s^{i+1} - s^i\|_2. \quad (13)$$

■

Using the smoothness property of the potential function established in Lemma 2, the progress made by Algorithm 1 at iteration  $i$  satisfies:

$$\Phi(s^{i+1}) - \Phi(s^i) \geq \frac{1}{2\alpha} \|\nabla\Phi(s^i)\|_2^2, \quad (14)$$

which follows from the standard descent lemma for  $\alpha$ -smooth functions. By the stopping rule, the algorithm continues only while  $\|\nabla\Phi(s^i)\|_\infty \geq \epsilon$ ; since  $\|\cdot\|_2 \geq \|\cdot\|_\infty$ , we have  $\|\nabla\Phi(s^i)\|_2 \geq \epsilon$  for all iterations before termination. Hence,

each iteration yields an improvement of at least:

$$\Phi(s^{i+1}) - \Phi(s^i) \geq \epsilon^2/2\alpha. \quad (15)$$

As  $\Phi(s)$  is monotonically non-decreasing and upper-bounded, the cumulative increase of the potential function over all iterations cannot exceed its feasible range ( $\Phi_{\max} - \Phi_{\min}$ ):

$$\sum_{i=0}^{I-1} [\Phi(s^{i+1}) - \Phi(s^i)] \leq \Phi_{\max} - \Phi_{\min}, \quad (16)$$

where  $\Phi_{\max} = \max_{s \in \mathcal{S}} \Phi(s)$  denotes the maximum value of the potential function over the feasible strategy set and  $\Phi_{\min} = \Phi(s^0)$  represents the value of the potential function corresponding to the initial equal resource allocation. Substituting the per-iteration improvement bound yields:

$$I \cdot \epsilon^2/2\alpha \leq \Phi_{\max} - \Phi_{\min}, \quad (17)$$

therefore, the number of iterations  $I$  required for convergence is bounded by:

$$I \leq I_{\max} = \frac{2\alpha(\Phi_{\max} - \Phi_{\min})}{\epsilon^2}. \quad (18)$$

We evaluate impact of  $\epsilon$  on  $I$  in Section VII-B1.

## V. PROPOSED JOINT ROUTE SELECTION AND RESOURCE ALLOCATION

This section presents our greedy solution to the route selection and resource allocation problem defined in (3) and illustrates interdependencies of joint optimization process.

### A. Proposed greedy algorithm

We propose a greedy approach to solve the problem (3) at reasonable complexity, summarized in Algorithm 2. The algorithm first computes the direct delivery durations  $t_{m,f,r}^{\text{dir}}$  for each content  $f$  requested by the  $m$ -th UE via the  $r$ -th direct route (line 1), and then constructs the direct delivery duration matrix  $\mathbf{T}^{\text{dir}}$  from the computed durations (line 2). For any base station that does not have the requested content in its cache, the corresponding entries in  $\mathbf{T}^{\text{dir}}$  are set to  $\infty$ , thereby ensuring that only feasible direct delivery options are considered. Then, the route selection indicator  $x_{m,f,r}$  is initialized to 0 for all  $m$  and  $r$  (line 3). Next, the algorithm selects the  $r$ -th direct delivery route for the  $m$ -th requesting UE that provides the minimum delivery duration  $t_{m,f,r}^{\text{dir}}$  from  $\mathbf{T}^{\text{dir}}$  (i.e., Algorithm 2 finds  $\min(\mathbf{T}^{\text{dir}})$  (line 5). Once the route is selected, the corresponding route selection indicator  $x_{m,f,r}$  is set to 1 (line 6), and the  $m$ -th row of  $\mathbf{T}^{\text{dir}}$  is set to  $\infty$  to prevent this UE from being assigned to another direct route (line 7). Then, the algorithm updates all remaining positive entries in  $\mathbf{T}^{\text{dir}}$  (if any) that involve the serving base station of the selected  $r$ -th direct delivery route by reallocating resources using the game-theoretic method described in Algorithm 1 (line 8). This process (lines 5-8) continues until all requesting UEs have been assigned a direct delivery route. For notational clarity, the initially assigned direct delivery route of the  $m$ -th requesting UE is denoted as  $r^{\text{dir}}$ .

---

### Algorithm 2 Joint route selection and resource allocation algorithm

---

- 1: Compute  $t_{m,f,r}^{\text{dir}}$  for all feasible direct routes  $r^{\text{dir}} \forall m$
  - 2: Create direct delivery matrix  $\mathbf{T}^{\text{dir}}$
  - 3: Set  $x_{m,f,r} = 0, \forall m, r$
  - 4: **repeat**
  - 5:      $t_{m,f,r}^{\text{dir}} \leftarrow \arg \min(t_{m,f,r}^{\text{dir}}) \in \mathbf{T}^{\text{dir}}$
  - 6:      $x_{m,f,r} = 1$
  - 7:     Set  $n$ -th row in  $t_{m,f,r}^{\text{dir}}$  to  $\infty$
  - 8:     Update  $t_{m,f,r}$  with proposed resource allocation
  - 9: **until** all UEs requesting content has assigned a direct route
  - 10: Calculate  $G_{m,f,r}, \forall m, r$
  - 11: Create matrix  $\mathbf{G}$
  - 12: **while**  $\max(G_{m,f,r}) > 0$  **do**
  - 13:      $\{m, f, r\} \leftarrow \arg \max(G_{m,f,r}) \in \mathbf{G}$
  - 14:      $x_{m,f,r} = 1$
  - 15:     Set  $m$ -th row in  $\mathbf{G}$  to 0
  - 16:     Update  $\mathbf{G}$  using (19) with proposed resource allocation
  - 17: **end while**
- 

In the next stage, the Algorithm 2 selects multi-hop routes for each requesting UE provided that content delivery would be decreased. To this end, we define the multi-hop gain  $G_{m,f,r}$ , which quantifies the potential reduction in delivery duration if the  $m$ -th UE requesting the  $f$ -th content would select the  $r$ -th multi-hop route instead of its currently assigned  $r^{\text{dir}}$ -th direct route. The gain  $G_{m,f,r}$  is expressed as:

$$G_{m,f,r} = \begin{cases} t_{m,f,r}^{\text{dir}} - t_{m,f,r}^{\text{mh}} - \Delta t_r, & \text{if } G_{m,f,r} > 0 \\ 0, & \text{otherwise} \end{cases} \quad (19)$$

where  $t_{m,f,r}^{\text{dir}}$  is the delivery duration of the  $f$ -th content to the  $m$ -th UE via its initially assigned  $r^{\text{dir}}$ -th direct route,  $t_{m,f,r}^{\text{mh}}$  is the delivery duration via the  $r$ -th multi-hop route, and  $\Delta t_r$  accounts for the potential prolongation in content delivery duration experienced by other UEs as a result of selecting the  $r$ -th multi-hop route for the  $m$ -th UE. This effect arises because selecting the  $r$ -th multi-hop route for the  $m$ -th UE requires reallocating both transmission power at the nodes in the  $r$ -th route and bandwidth across all simultaneously transmitted contents. Due to interdependencies in resource allocation across transmitting nodes, these re-allocations may also affect the resource allocation at nodes outside the  $r$ -th route, thereby influencing the delivery duration of other requesting UEs. However, if the selected  $r$ -th multi-hop route does not involve any transmitting nodes that are part of previously selected multi-hop routes for other UEs, then  $\Delta t_r$  is 0, as the resource allocation at the nodes in the  $r$ -th route does not affect the resource allocation at the nodes serving these other UEs. If the resulting  $G_{m,f,r}$  in (19) is positive, selecting the  $r$ -th multi-hop route instead of the  $r^{\text{dir}}$ -th direct route is beneficial in terms of reducing the overall content delivery duration. Otherwise, the  $r^{\text{dir}}$ -th direct route remains preferred, and the  $G_{m,f,r}$  is set to 0.

In the next step, the multi-hop gains between all requested UEs and transmission routes are inserted into a multi-hop gain matrix  $\mathbf{G}$ , which is of dimension  $M \times (R - U - 1)$  (excluding

direct routes), as indicated in line 11. Then, the Algorithm 2 selects the maximum multi-hop gain in  $\mathbf{G}$ , as this selection decreases the overall content delivery duration by the highest degree (i.e., Algorithm 2 finds  $\max(G_{m,f,r})$ , line 13). Then,  $x_{m,f,r}$  is set to 1, indicating that the  $m$ -th UE receives the  $f$ -th content via the selected  $r$ -th multi-hop route instead of the previously assigned  $r^{\text{dir}}$ -th direct route, for which  $x_{m,f,r^{\text{dir}}}$  is set to 0 to reflect this update (line 14). Next, all entries in the  $m$ -th row of  $\mathbf{G}$  are set to 0, as this UE has now committed to a specific transmission route for delivering the requested content and cannot select any multi-hop route (line 15).

Next, Algorithm 2 updates the remaining positive entries in  $\mathbf{G}$  (if any) that correspond to routes involving any nodes that are part of all selected multi-hop transmission routes, in accordance with (19) (line 16). This update is necessary because the selection of each new multi-hop route affects the resource allocation across all transmitting nodes involved in previously selected routes, as explained earlier. Thus, the net reduction in overall content delivery duration achieved by selecting a new multi-hop route must outweigh any potential increase in delivery duration for other UEs that have already selected multi-hop transmission routes. Therefore, this effect is reflected in the recalculation of  $\mathbf{G}$  via  $\Delta t_r$  with the updated resource allocation. The Algorithm 2 repeats lines 13–16 until no positive entries remain in the multi-hop gain matrix  $\mathbf{G}$ . In each iteration, the algorithm selects the transmission route with the highest multi-hop gain and updates the resource allocation accordingly. Note that requesting UEs that do not select a multi-hop transmission route retain their initially assigned direct delivery routes.

Algorithm 2 has the worst case time complexity of  $\mathcal{O}(M^2(R-U-1))$ , as in the first step  $M(R-U-1)$  values has to be checked, in the second step  $(M-1)(R-U-1)$  values are checked, until  $(R-U-1)$  values are checked.

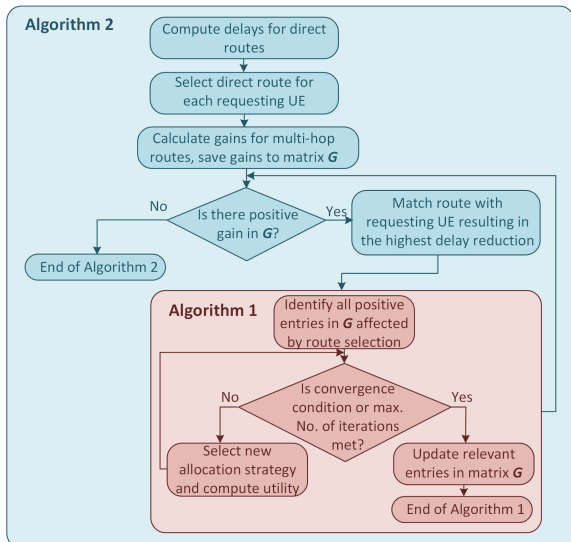


Fig. 3: High-level illustration of joint optimization and inter-dependencies between algorithms.

### B. Summary of joint optimization process

The inter-dependencies between Algorithms 1 and 2 and whole iteration/update process is summarized into the following steps (see Fig. 3): *i*) for each requesting UE and for every direct route from the content-providing node (GBS or UAV) that stores the requested content, Algorithm 2 computes the resulting content delivery duration; *ii*) Algorithm 2 selects the direct route that yields the minimum content delivery duration for each requesting UE; *iii*) for each requesting UE and each candidate multi-hop route, Algorithm 2 computes the multi-hop gain and stores all gains in the multi-hop gain matrix  $\mathbf{G}$ ; *iv*) Algorithm 2 checks whether the multi-hop gain matrix  $\mathbf{G}$  contains at least one positive element; if not, routes for delivering the requested contents have been selected for all requesting UEs (i.e., Algorithm 2 terminates), otherwise *v*) Algorithm 2 matches the requesting UE and the multi-hop route that provides the highest reduction in the content delivery duration and updates the route of this UE to the selected multi-hop route; *vi*) after that, Algorithm 1 identifies all positive entries in matrix  $\mathbf{G}$  that correspond to the routes whose nodes are affected by the newly selected multi-hop route; *vii*) at each iteration, Algorithm 1 checks whether the convergence condition is satisfied or the maximum number of iterations has been reached; if neither condition holds, Algorithm 1 selects a new resource allocation strategy (transmission power and bandwidth) for the affected nodes and updates their allocations, otherwise Algorithm 1 updates the corresponding entries of  $\mathbf{G}$  and process goes back to step *iv*).

## VI. IMPLEMENTATION ASPECTS OF THE PROPOSAL

This section describes several implementation aspects and potential limitations of the proposed concept.

The proposed framework requires a central coordinator, potentially implemented at the GBS, to execute the joint route selection and resource allocation algorithm. This coordinator performs three tasks, each resulting in a communication of computational overhead:

1) *Acquiring network-wide information*: To make apprised decisions, the coordinator should be aware of user content requests, the caching status of UAVs, and channel quality between nodes. Most of this information is already present in practical cellular systems. Namely, the UE content requests are naturally reported to the network, channel quality is periodically measured and reported, and the caching status of the UAVs can be reported to the GBS via standard control signaling over the air interface. Of course, obtaining channel quality for all possible node pairs in a traditional way would lead to substantial signaling overhead. However, the channel quality can be predicted by many existing artificial intelligence/machine learning-driven channel estimation approaches, as surveyed in [38]. For instance, channel quality prediction framework proposed for general environment in [39][40] and further optimized and validated for indoor environment in [41] requires no additional signaling overhead, as the channel quality prediction relies on information already available in the mobile networks.

2) *Execution of the proposed framework*: After the coordinator obtains all necessary information, the proposed algorithms

are executed, resulting in additional computational overhead. The computational overhead of the proposed framework remains practically manageable for two main reasons. First, the greedy algorithm based-route selection algorithm is explicitly designed to keep the computational complexity manageable. One of the main reasons for introducing the multi-hop gain is to prune multi-hop routes that are not promising in terms of reducing the content delivery duration. By eliminating multi-hop routes that cannot outperform the direct delivery, the algorithm reduces the number of route evaluations and resource allocation updates to mitigate the computational overhead and improves scalability to larger networks. Second, as we show in Section VII, the number of iterations required by the iterative resource allocation algorithm remains relatively small (few iterations per UE) across the considered range of requesting UEs. This indicates that the centralized controller can perform the required computations within the time scale of content delivery, so that the computational effort remains practically manageable in the real networks.

3) *Distribution of decisions to relevant nodes*: Last, after the route selection and the resource allocation are performed, the coordinator distributes the results to the UAVs and the RUEs, leading to some additional signaling overhead at the system level. Nevertheless, this overhead can be accommodated within existing cellular network control channels, since the framework builds on standard measurement reports and configuration or scheduling messages that are already exchanged at comparable time scales.

The computation and communication overhead can be further minimized by extension of the proposal towards partially- or fully- distributed by leveraging multi-agent or federated learning techniques for local route selection and resource allocation decisions at the UAVs and the RUEs, following distributed learning paradigms, such as those in [42], [43].

Last practical aspect is related to the tuning of parameter  $\epsilon$ . A smaller  $\epsilon$  leads to more precise solutions but requires a higher number of iterations, increasing computational complexity. Conversely, a larger  $\epsilon$  reduces computational overhead at the expense of a marginal decrease in optimality. In Section VII, we analyze the impact of  $\epsilon$  on both convergence speed and average content delivery duration, providing practical guidelines for selecting  $\epsilon$  in real-time network deployments. In practical systems,  $\epsilon$  can be dynamically adjusted by the concept known as self-organizing networks (SON) and by machine learning methods, enabling the network to autonomously tune this parameter based on system needs, thus optimizing the trade-off between performance and computational efficiency.

## VII. SIMULATION DESCRIPTION

This section first presents the simulation scenario and settings, followed by a description of the competitive algorithms. Then, the simulation results and discussion is given.

### A. Simulation Scenario and Competitive Schemes

To evaluate the performance of the proposal, we conduct simulations using MATLAB. The code of implemented pro-

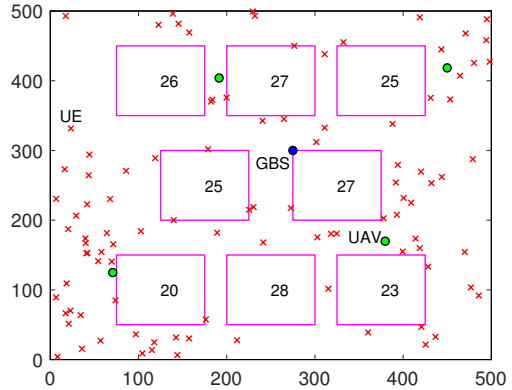


Fig. 4: Example simulation scenario in an urban area, where buildings are represented by pink rectangular blocks.

TABLE I: Simulation parameters

Parameter	Value
Area size	500 × 500 m <sup>2</sup>
Carrier frequency	2 GHz
Bandwidth ( $B$ )	100 MHz
# of UAVs ( $U$ ), UEs ( $N$ ), RUE ( $N - M$ )	1-4; 80-230; 50-200
Max. Tx power of GBS ( $P_{max}^{GBS}$ ); UAV ( $P_{max}^{UAV}$ ); UE ( $P_{max}^{RUE}$ )	30; 30; 23 dBm
Antenna gain of the GBS, and UAVs	3 dBm
Height of the GBS, UAVs, UEs	35; 100; 1.5 m
Storage size of GBS ( $F$ ) and UAVs ( $F_u$ )	50; 10 files
Content size ( $S_f$ )	1-10 Mbits
Noise spectral density ( $\sigma$ )	-174 dBm/Hz
Background interference ( $I_b$ )	$U(-140, -120)$ dBm/Hz

posal is available at GitLab<sup>1</sup>. We consider a 500 × 500 m<sup>2</sup> simulated area with multiple buildings to emulate an urban environment (see Fig. 4). The height of each building is randomly generated between 20 and 29 m [44]. The GBS is placed at a fixed location on the upper-left corner of the building closest to the center of the simulated area, as illustrated in Fig. 4. To provide aerial coverage, we deploy up to four UAVs to the positions determined by K-means algorithm according to the locations of the UEs, as in [45]. The UAVs are assumed to operate at an altitude of 100 m [46].

Further, we consider up to 230 UEs uniformly distributed throughout the area and located outdoor. Indoor users are not explicitly modelled in the network, since indoor penetration loss and deep shadow fading caused by building walls significantly attenuate the UAV signals in indoor environments. In addition, the limited battery life-time of the UAVs makes the UAV-assisted content delivery inefficient for indoor users [47]. Out of all UEs, up to 30 request specific content, while the remaining serve as the potential RUEs to assist in content dissemination. Each requested content has a different size, varying between 1 and 10 Mbit.

The channel between any two nodes (UEs, UAVs, and GBS) follows a well-established model for UAV communication

<sup>1</sup>Code of the proposal in Matlab: <https://gitlab.fel.cvut.cz/mobile-and-wireless/codes/publications/joint-route-selection-and-radio-resources-allocation-for-caching-in-multi-hop-networks>

in urban environment, as introduced in [48]. This model accounts for the presence of buildings that may obstruct the LoS path between a transmitter and a receiver. In such cases, each obstructing building introduces an additional 20 dB of attenuation [49]. Since the GBS and UAVs are located above rooftop level, they are assumed to maintain LoS links with each other. In contrast, links between the GBS/UAVs and the UEs may be blocked by one or more buildings, depending on the relative positions of nodes. In addition, the channel is affected by small-scale fading modeled as circularly symmetric complex Gaussian (CSCG) random variable with zero mean and unit variance [50]. We exploit Rayleigh fading model with the maximum Doppler shift set to 10 Hz, which corresponds to a pedestrian speed of approximately 1.5 m/s at a carrier frequency of 2 GHz. In addition, channel estimation errors are also modeled by CSCG [26] with variance proportional to the squared magnitude of the true gain  $\epsilon_g^2 = \delta_g^2 |g_{k,k'}|^2$ , where we set  $\delta_g = 0.3$  resulting in the channel estimation/prediction errors typically varying between  $-5$  and  $5$  dB. Further, we assume the background interference uniformly distributed between  $-140$  to  $-120$  dBm/Hz. This corresponds to a very strong interference from neighboring cells to investigate performance of the proposal in challenging and adverse environments expected in future dense networks.

The simulation is repeated over 100 simulation drops, each involves randomly generating the building heights, all UEs locations based on which the locations of all UAVs is also determined, and the set of contents cached at the UAVs. After that, the simulation results are averaged out over all simulation drops to reduce the impact of randomness. The main simulation parameters are summarized in Table I.

The primary performance metric evaluated in this work is the content delivery duration, including average values and distribution of delivery durations captured by cumulative distribution function (CDF). We also assess the convergence characteristics of the proposed resource allocation algorithm by reporting the average number of iterations per UE needed to reach a specified convergence threshold. The proposed solution is compared with the following state-of-the-art algorithms:

- Route selection with equal power split (*RS + eq. PS*) [15] – The greedy algorithm jointly handles route selection and power allocation with an equal power split.
- Route selection with power allocation (*RS + PA*) [16] – The greedy algorithm jointly handles route selection and power allocation using a heuristic power allocation algorithm.
- *Iterative* [51] – This algorithm applies an alternating optimization scheme, where greedy route selection is performed first, followed by Lagrangian-based power allocation, then greedy Kuhn-Munkres-based bandwidth allocation, and finally another round of power optimization. The updated solution from each step is used in the subsequent step, and these steps are repeated sequentially until convergence.
- *DPA-D2D* [52] – This algorithm first selects routes via a stable-matching mechanism and, then, determines the transmission power and bandwidth allocation in a single pass, without an outer iterative loop that jointly refines

all variables until convergence.

## B. Simulation Results

In this section, we present and discuss the simulation results, including convergence analysis, and the impact of the number of requesting UEs, number of UAVs, number of RUEs, and the Zipf exponent on average content delivery duration and the distribution of delivery durations.

1) *Convergence analysis:* Fig. 5(a) illustrates the average number of iterations required for the convergence of the proposed resource allocation algorithm as the number of requesting UEs increases. We assume different values of convergence threshold  $\epsilon$ , which defines the optimality condition for terminating the iterative optimization. As the number of requesting UEs increases, resource allocation process requires more iterations to reallocate resources among a larger number of contents. Moreover, smaller  $\epsilon$  values (e.g.,  $10^{-5}, 10^{-6}$ ) result in a significantly higher number of iterations compared to larger  $\epsilon$  values (e.g.,  $10^{-1}, 10^{-2}$ ). This is because tighter convergence threshold enforces more precise optimization, requiring additional updates to reach the desired optimality condition. However, as shown in Fig. 5(b), the difference in content delivery durations between smaller and larger  $\epsilon$  values remains marginal, even for higher numbers of requesting UEs.

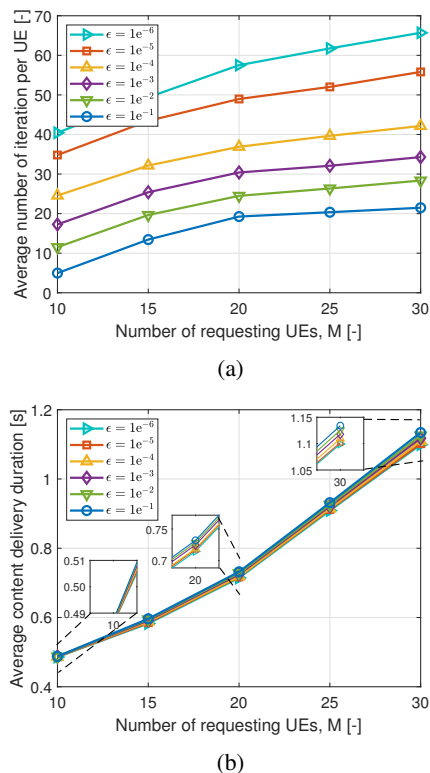
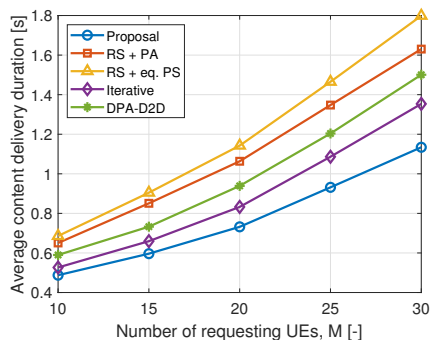


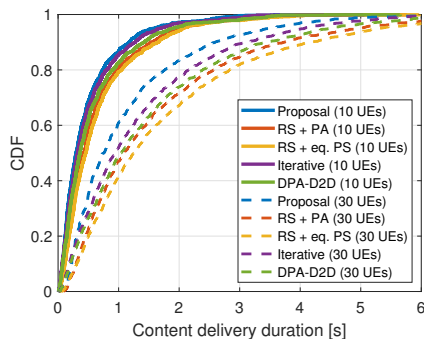
Fig. 5: Impact of convergence threshold ( $\epsilon$ ) on the proposed resource allocation algorithm (Zipf exponent  $\lambda = 0.5$ , number of UAVs  $U = 4$ , number of UEs  $N = 100$ ): (a) average number of iterations required for convergence versus number of requesting UEs, (b) average content delivery duration versus number of requesting UEs.

Specifically, for 30 requesting UEs, the reduction in average content delivery duration when using  $\epsilon = 10^{-6}$  instead of  $\epsilon = 10^{-1}$  is minimal (approximately 3%), while the number of iterations required for convergence increases by more than three times. This indicates that the proposed algorithm maintains high efficiency and robustness even with a less strict convergence threshold. Therefore, a larger  $\epsilon$  value such as  $10^{-1}$  provides an effective trade-off, achieving near-optimal performance while significantly reducing computational complexity. Accordingly, we set  $\epsilon = 10^{-1}$  in the following simulations. Furthermore, the results are encouraging in promoting the proposed algorithm in real networks. Even with relatively high number of UEs simultaneously requesting the contents, the number of iterations is very low, first increasing linearly with the number of requesting UEs and later even saturating.

2) *Impact of number of requesting UEs*: Fig. 6(a) presents the average content delivery duration achieved by different algorithms for varying numbers of requesting UEs. The average content delivery duration for all schemes rises with the number of requesting UEs in the system. The increase is due to two main factors: *i*) the transmission resources (power and bandwidth) are divided among a larger number of contents and *ii*) fewer relays remain available, as there are  $N - M$  UEs available for relaying. Still, the proposed algorithm consistently outperforms the benchmark algorithms and the performance gap increases with more requesting UEs.



(a)



(b)

Fig. 6: Impact of number of requesting UEs on: (a) average content delivery duration for varying number of requesting UEs ( $\lambda = 0.5$ ,  $U = 4$ ,  $N = 100$ ), (b) CDF for 10 and 30 requesting UEs under the same network settings.

The proposed algorithm reduces the average content delivery duration by up to 16.2%, 24.4%, 30.4%, and 37% compared to the *Iterative*, *DPA-D2D*, *RS + PA*, and *RS + eq. PS* schemes, respectively. The notable improvements over the *RS + PA* and *RS + eq. PS* schemes are attributed to their reliance on fixed bandwidth allocation, whereas the proposed algorithm jointly optimizes bandwidth and power allocations dynamically, leading to more efficient resource utilization and reduced content delivery durations. Additionally, the gain over the *Iterative* and *DPA-D2D* algorithm arises from our holistic joint optimization of route selection alongside power and bandwidth allocation, as opposed to the *Iterative* and *DPA-D2D* algorithms' sequential approach.

To provide further insights into the distribution of actual content delivery durations, we present the CDF of the delivery duration for each algorithm in Fig. 6(b). As shown in Fig. 6(b), the *RS + PA* and *RS + eq. PS* schemes, which employ fixed bandwidth allocation, exhibit a higher incidence of outliers compared to the proposed, *Iterative*, and *DPA-D2D* algorithms, all of which optimize bandwidth allocation as part of their solution. In addition, for the evaluated numbers of requesting UEs ( $M = 10$  and  $M = 30$ ), the proposed algorithm demonstrates more consistent content delivery durations compared to the *Iterative* and *DPA-D2D* algorithms. Specifically, the proposed algorithm enables approximately 97.2% and 83.3% of requesting UEs for 10 and 30 requesting UEs, respectively, to receive their content within 2 s. In comparison, for 10 requesting UEs, approximately 96.9%, 95.7%, 95.1%, and 94.2% of UEs receive their content within 2 s under the *Iterative*, *DPA-D2D*, *RS + PA*, and *RS + eq. PS* schemes, respectively. For 30 requesting UEs, these percentages decrease to approximately 77.7%, 73.8%, 71.7%, and 67.1% for the same schemes, respectively. The results confirm that the joint design of the proposed algorithm effectively reduces the content delivery duration compared to the *Iterative* and *DPA-D2D* algorithms.

3) *Impact of number of UAVs*: Fig. 7(a) illustrates the average content delivery duration for varying numbers of UAVs in the network. Since UAVs serve both as content providers and relaying nodes, variations in the number of UAVs have a significant impact on overall system performance. The average content delivery duration decreases as the number of UAVs increases due to three main factors: *i*) more UAVs are responsible for covering the same area, which generally reduces the distance between UAVs and requesting UEs; *ii*) a higher number of UAVs increases the likelihood that requesting UEs receive their content from nearby UAVs; and *iii*) increased UAV density brings UAV relays closer both to requesting UEs and the GBS. The proposed algorithm outperforms all benchmark schemes across all evaluated numbers of UAVs. With one UAV in the network, the proposed algorithm achieves gains of 47%, 37.5%, 31.5%, and 22.6% compared to *RS + eq. PS*, *RS + PA*, *DPA-D2D*, and *Iterative* algorithms, respectively. When the number of UAVs increases to four, the gains are 37%, 30.4%, 24.4%, and 16.2% over *RS + eq. PS*, *RS + PA*, *DPA-D2D*, and *Iterative* algorithms, respectively. Moreover, these results highlight that even with a limited number of UAVs (i.e.,  $U = 1$ ), which represents a more economical

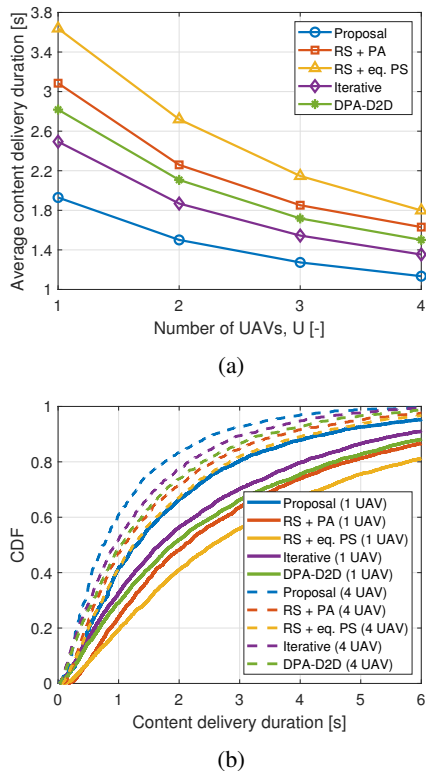


Fig. 7: Impact of number of UAVs on: (a) average content delivery duration versus number of UAVs ( $\lambda = 0.5$ ,  $N = 100$ ,  $M = 30$ ). (b) CDF for 1 and 4 UAVs under the same network settings.

deployment scenario for network operators, the proposed algorithm provides significant performance improvements.

Fig. 7(b) presents the CDF of content delivery duration for the proposed algorithm under two UAV deployment scenarios: with one UAV and four UAVs in the network. With four UAVs deployed, approximately 83.3% of contents are received within 2 s using the proposed algorithm, indicating a steeper and more favourable distribution compared to 67.1%, 71.7%, 73.8%, and 77.7% for the *RS + eq. PS*, *RS + PA*, *DPA-D2D*, and *Iterative* schemes, respectively. Similarly, with only one UAV, the proposed algorithm achieves 66.4% within 2 s, outperforming the *Iterative*, *DPA-D2D*, *RS + PA*, and *RS + eq. PS* schemes, which achieve only 56.3%, 51.9%, 48.1%, and 40.9% respectively. The results demonstrate that the proposed method not only reduces average delivery duration but also improves the distribution of delivery durations, leading to more consistent performance across the network.

Fig. 7(a) and 7(b) demonstrate that the reduction in the average content delivery duration achieved by the proposed algorithm over the benchmark schemes is particularly pronounced when fewer UAVs are deployed (i.e.,  $U = 1$ ). When there are few UAVs in the network, the number of content-providing nodes (i.e., GBS and UAVs) decreases. As a result, the existing UAVs (which also serve as relaying nodes) along with the GBS are utilized more frequently in the content delivery routes. This increased usage of the GBS and UAV(s) intensifies the interdependence between resource

allocation and route selection decisions, thereby increasing the optimization complexity. These results lead to two key conclusions. First, in the cache-enabled multi-hop networks, incorporating bandwidth allocation into the joint optimization framework instead of relying on fixed bandwidth allocation significantly reduces the content delivery duration. Second, the joint design of route selection, power allocation, and bandwidth allocation demonstrates greater performance gains in more challenging scenarios characterized by a limited number of UAVs. In these scenarios, the proposed joint design achieves lower content delivery durations compared to the iterative optimization approaches.

4) *Impact of number of RUEs*: Fig. 8(a) illustrates the average content delivery duration for varying RUEs in the network. As the number of the RUEs increases, more RUEs are available as relaying nodes, thus, enlarging the set of possible delivery routes. A larger set of delivery routes allows the algorithm to select more efficient routes for content delivery, thereby reducing the average content delivery duration. The proposed algorithm consistently achieves the lowest average content delivery duration across all evaluated numbers of RUEs. When the number of RUEs increases from 50 to 200, the gain of the proposed scheme over *RS + eq. PS* increases from 37.4% to 47%, and the gain over *RS + PA* increases from 30.6% to 37.5%. The performance gain of the proposal

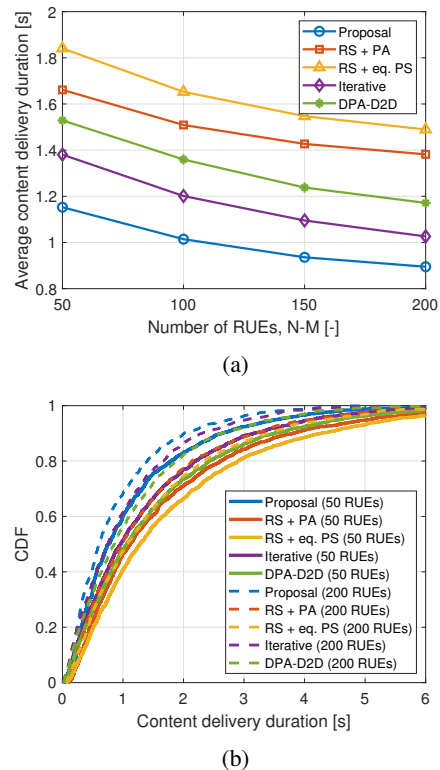


Fig. 8: Impact of the number of RUEs: (a) Average content delivery duration versus number of RUEs (Zipf exponent  $\lambda = 0.5$ , number of requesting UEs  $M = 30$ , number of UAVs  $U = 4$ ). (b) CDF for 50 and 200 RUEs under the same network settings.

with respect to  $RS + eq. PS$  and  $RS + PA$  increases, since the bandwidth allocation for  $RS + eq. PS$  and  $RS + PA$  is fixed and  $RS + eq. PS$  uses only equal power splitting.

Further, we can observe in Fig. 8(a) that the gain of the proposal compared to  $DPA-D2D$  remains roughly the same if the number of RUEs increases from 50 to 200 (change from 24.6% to 23.6%), while the gain over the *Iterative* scheme decreases from 16.5% to 12.8%. The reason why the gain over *Iterative* schemes decreases with more available RUEs is that the number of multi-hop routes yielding low content delivery durations also increases. As a result, the probability that the delivery routes of different requesting UEs share the same transmitting nodes decreases, thus reducing the interdependencies between route selection and resource allocation decisions. Still, up to 200 RUEs is rather optimistic in our confined area since only a subset of users will be usually willing to act as the relays for others due to battery constraints and/or limited device capability despite if some incentives will be given to them.

Fig. 8(b), capturing CDF for 50 and 200 RUEs, indicates that with more RUEs, a higher fraction of requesting UEs experiences low content delivery durations. This outcome is expected, because more potential relaying routes become available with more RUEs yielding shorter delivery durations. For the cases of 50 and 200 RUEs, the proposed algorithm enables approximately 83.0% and 89.9% of users to receive their requested content within 2 s, respectively. In comparison, *Iterative* scheme achieves 77.0% and 86.5%, the  $DPA-D2D$  achieves 73.5% and 82.1%, the  $RS + PA$  achieves 71.0% and 77.6%, and the  $RS + eq. PS$  achieves 66.4% and 74.6% for the same scenarios.

5) *Impact of Zipf exponent*: This section analyses the impact of the Zipf exponent ( $\lambda$ ) on content delivery duration. The  $\lambda$  quantifies the unevenness in the distribution of UEs requests among available contents, which affects the subset of contents UAVs cache and, in turn, the delivery duration of requested contents. Note that, in practice, the  $\lambda$  is determined by users' behaviour and content popularity dynamics and is not controllable by the system.

Comparison across different  $\lambda$  settings in Fig. 9(a) reveals that average content delivery duration decreases as the  $\lambda$  increases for all schemes. This is because a higher  $\lambda$  means that user requests are focused on a smaller set of highly popular contents, increasing the likelihood that these popular contents are cached at UAVs located near the requesting UEs. Consequently, caching these popular contents at UAVs' storage closer to the requesting UEs reduces delivery distances and durations, thereby improving overall system performance. If the  $\lambda$  is set to 0.25, the proposed algorithm reduces the average content delivery duration by 17.68%, 24.86%, 30.16%, and 37.34% compared to the *Iterative*,  $DPA-D2D$ ,  $RS + PA$ , and  $RS + eq. PS$  schemes, respectively. Meanwhile, as the  $\lambda$  rises to 1, the gains of the proposed algorithm compared to the  $RS + PA$  and  $RS + eq. PS$  schemes increase to 34.03%, and 39.59%, respectively, while the gain compared to the *Iterative* and  $DPA-D2D$  algorithms slightly decreases to 13.43% and 23.11%, respectively.

Fig. 9(b) illustrates the CDF of content delivery duration

under two different  $\lambda$  settings,  $\lambda = 0.25$  and  $\lambda = 1$ , highlighting the impact of content popularity distribution on delivery performance. For  $\lambda = 0.25$ , the distribution of content delivery durations is wider and more variable across all algorithms compared to  $\lambda = 1$ , indicating less consistent delivery performance in scenarios with more diverse content requests. This is because in settings with low  $\lambda$  (i.e.,  $\lambda = 0.25$ ), content requests are more diverse, reducing the likelihood that requested contents are cached at nearby UAVs. Consequently, the content requested by UEs is predominantly delivered from the GBS, which allocates its transmission resources among a higher number of contents or from distant UAVs, thereby resulting in increased content delivery duration. For  $\lambda = 0.25$ , approximately 79.5% of contents are delivered within 2 s for the proposal, outperforming the *Iterative*,  $DPA-D2D$ ,  $RS + PA$ , and  $RS + eq. PS$  schemes, which achieve 72.1%, 69.0%, 66.8%, and 61.8%, respectively. When  $\lambda = 1$ , approximately 90.0% of contents are received within 2 s using the proposed algorithm, compared to 87.2%, 83.8%, 79.5%, and 77.7% for the *Iterative*,  $DPA-D2D$ ,  $RS + PA$ , and  $RS + eq. PS$  schemes, respectively.

### VIII. CONCLUSION

In this paper, we have investigated a joint route selection, transmission power, and bandwidth allocation problem to minimize the sum content delivery duration in cache-enabled multi-hop networks. To address this joint problem,

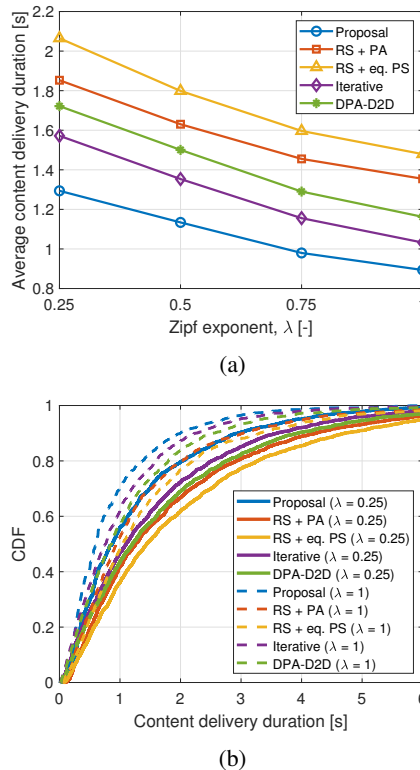


Fig. 9: Impact of Zipf exponent on: (a) average content delivery duration ( $N = 100$ ,  $M = 30$ ,  $U = 4$ ), (b) CDF of content delivery duration for  $\lambda = 0.25$  and  $\lambda = 1$  under the same network settings.

we have first modeled joint power and bandwidth allocation as a cooperative resource allocation game, proved that it is a potential game, and solved it using an iterative algorithm based on an approximate better-response mechanism. Then, we have proposed a greedy algorithm tailored to jointly manage route selection and resource allocation, explicitly capturing their interdependencies. In this algorithm, transmission routes are sequentially selected for each content, with the resource allocations of the involved nodes updated to reflect their impact on the delivery duration of contents whose routes have not yet been determined. Simulation results demonstrate that the proposed scheme reduces the average content delivery duration by 23.2% if compared to the best performing state-of-the-art scheme.

The proposed framework can be further extended towards UAV trajectory optimization, by finding proper incentives to relays, or by extension towards machine learning-based distributed approach.

## REFERENCES

- [1] L. Li, G. Zhao, and R. Blum, "A Survey of Caching Techniques in Cellular Networks: Research Issues and Challenges in Content Placement and Delivery Strategies," *IEEE Commun. Surv. Tutor.*, vol. 20, no. 3, pp. 1710-1732, 2018.
- [2] T. Duong *et al.*, "UAV caching in 6G networks: A Survey on models, techniques, and applications" *Physical Communication*, vol. 51, pp. 101532, 2022.
- [3] P. Mach, and Z. Becvar, "Device-to-device relaying: Optimization, performance perspectives, and open challenges towards 6G networks," *IEEE Commun. Surv. Tutor.*, vol. 24, no. 3, pp. 1336-1393, 2022.
- [4] J. Ji *et al.*, "Joint trajectory design and resource allocation for secure transmission in cache-enabled UAV-relaying networks with D2D communications," *IEEE Internet Things J.*, vol. 8, no. 3, pp. 1557-1571, 2020.
- [5] M. Al-Abiad, M. Hassan, and M. Hossain, "Throughput Maximization of Network-Coded and Multi-Level Cache-Enabled Heterogeneous Network," *IEEE Trans. Veh. Technol.*, vol. 70, no. 10, pp. 11039-11043, 2021.
- [6] A. Douik *et al.*, "Mode selection and power allocation in multi-level cache-enabled networks," *IEEE Commun. Lett.*, vol. 24, no. 8, pp. 1789-1793, 2020.
- [7] B. Tian *et al.*, "UAV-assisted wireless cooperative communication and coded caching: a multiagent two-timescale DRL approach," *IEEE Trans. Mob. Comput.*, 2023.
- [8] X. Qi *et al.*, "Joint power-trajectory-scheduling optimization in a mobile UAV-enabled network via alternating iteration," *China Communications*, vol. 19, no. 1, pp. 136-152, 2022.
- [9] W. Wang *et al.*, "Joint cooperative caching and power control for UAV-assisted internet of vehicles," *Scientific Reports*, vol. 14, no. 1, pp. 9341, 2024.
- [10] P. Qin *et al.*, "Latency Minimization Resource Allocation and Trajectory Optimization for UAV-Assisted Cache-Computing Network with Energy Recharging," *IEEE Trans. Commun.*, 2025.
- [11] D. Wang *et al.*, "Deep Reinforcement Learning for Caching in D2D-Enabled UAV-Relaying Networks," *IEEE ICC*, 2021, pp. 635-640.
- [12] L. Luo, R. Sun, R. Chai, and Q. Chen, "Cost-Efficient UAV Deployment and Content Placement for Cellular Systems With D2D Communications," *IEEE Systems Journal*, 2023.
- [13] J. Yao, T. Han, and N. Ansari, "On mobile edge caching," *IEEE Commun. Surv. Tutor.*, vol. 21, no. 3, pp. 2525-2553, 2019.
- [14] X. Gu, and G. Zhang, "A survey on UAV-assisted wireless communications: Recent advances and future trends," *Computer Communications*, vol. 208, pp.44-78, 2023.
- [15] E. Gures, and P. Mach, "Joint Route Selection and Power Allocation in Multi-Hop Cache-Enabled Networks," *IEEE WCNC*, 2024, pp. 1-6.
- [16] E. Gures, and P. Mach, and Z. Becvar, "Dynamic Transmission Power Allocation for Cache-enabled Multi-hop Networks," *IEEE WCNC*, 2025, pp. 1-6.
- [17] L. Wang, Q. Zhou, and Y. Shen, "Computation efficiency maximization for UAV-assisted relaying and MEC networks in urban environment," *IEEE Trans. Green Commun. Netw.*, vol. 7, no. 2, pp. 565-578, 2022.
- [18] Y. Wang *et al.*, "Joint Positioning and Computation Offloading in Multi-UAV MEC for Low Latency Applications: a Proximal Policy Optimization Approach," *IEEE Trans. Mobile Comput.*, 2025.
- [19] C. Liu *et al.*, "URLLC-aware proactive UAV placement in Internet of Vehicles," *IEEE Trans. Intell. Transp. Syst.*, vol. 25, no. 8, pp. 10446-10451, 2024.
- [20] Z. Becvar, M. Nikooroo, and P. Mach, "On energy consumption of airship-based flying base stations serving mobile users," *IEEE Trans. Commun.*, vol. 70, no. 10, pp. 7006-7022, 2022.
- [21] L. Breslau *et al.*, "Web caching and Zipf-like distributions: Evidence and implications," *IEEE INFOCOM*, vol. 1, pp. 126-134, 1999.
- [22] B. Liu *et al.*, "Dynamic cache placement and trajectory design for UAV-assisted networks: A two-timescale deep reinforcement learning approach," *IEEE Trans. Veh. Technol.*, vol. 73, no. 4, pp. 5516-5530, 2023.
- [23] W. Tang, H. Zhang, and J. Peng, "Performance analysis of cooperative caching and transmission diversity in cache-enabled UAV networks," *IEEE Trans. Wirel. Commun.*, vol. 23, no. 5, pp. 4411-4423, 2023.
- [24] X. Gao, X. Wang, and Z. Qian, "Probabilistic Caching Strategy and TinyML-Based Trajectory Planning in UAV-Assisted Cellular IoT System," *IEEE Internet Things J.*, vol. 11, no. 12, pp. 21227-21238, 2024.
- [25] P. Mach, Z. Becvar, and M. Nikooroo, "Multi-hop relaying with mixed half and full duplex relays for offloading to mec," *IEEE Globecom Workshops*, pp. 558-564, 2023.
- [26] Z. Zhu *et al.*, "Robust beamforming design for STAR-RIS-aided secure SWIPT system with bounded CSI error," *IEEE Trans. Green Commun. Netw.*, vol. 8, no. 3, pp. 968-977, 2024.
- [27] X. Huang *et al.*, "Outage Constrained Design for RIS-Assisted Integrated Sensing and Communication Systems," *IEEE Commun. Lett.*, vol. 29, no. 5, pp. 1037-1041, 2025.
- [28] G. Wang *et al.*, "Green Cell-Free Massive MIMO: An Optimization Embedded Deep Reinforcement Learning Approach," *IEEE Trans. Signal Process.*, 2024.
- [29] N. Sawyer, and D. Smith, "Flexible resource allocation in device-to-device communications using stackelberg game theory," *IEEE Trans. Commun.*, vol. 67, no. 1, pp. 653-667, 2018.
- [30] S. Fu *et al.*, "Joint power allocation and 3D deployment for UAV-BSS: A game theory based deep reinforcement learning approach," *IEEE Trans. Wirel. Commun.*, vol. 23, no. 1, pp. 736-748, 2023.
- [31] Y. Song, C. Zhang, and Y. Fang, "Joint channel and power allocation in wireless mesh networks: A game theoretical perspective," *IEEE J. Sel. Areas Commun.*, vol. 26, no. 7, pp. 1149-1159, 2008.
- [32] P. Duarte *et al.*, "On the partially overlapped channel assignment in wireless mesh network backbone: A game theoretic approach," *IEEE J. Sel. Areas Commun.*, vol. 30, no. 1, pp. 119-127, 2011.
- [33] D. Monderer, and L. Shapley, "Potential games," *Games and economic behavior*, vol. 14, no. 1, pp. 124-143, 1996.
- [34] J. Bai *et al.*, "EMI Characteristics Informed JSPA-BR Approach for Sensing, Networking and Computing Integrated Aerial IoT Applications," *IEEE Internet Things J.*, 2025.
- [35] X. Yang *et al.*, "Joint grouping and offloading in NOMA-assisted multi-MEC IoT systems," *IEEE Globecom*, pp. 5699-5704, 2022.
- [36] A. Abrardo *et al.*, "Distributed power allocation for D2D communications underlying/overlying OFDMA cellular networks," *IEEE Trans. Wirel. Commun.*, vol. 16, no. 3, pp. 1466-1479, 2016.
- [37] Z. Shuang *et al.*, "Joint beam scheduling and power optimization for beam hopping LEO satellite systems," *China Communications*, 2024.
- [38] Y. Gao, Z. Lu, X. Wu, W. Yu, S. Liu, and J. Du, "AI-Driven Channel State Information (CSI) Extrapolation for 6G: Current Situations, Challenges, and Future Research," *IEEE Communications Surveys and Tutorials*, vol. 28, pp. 4485-4518, 2026.
- [39] M. Najla, Z. Becvar, P. Mach, and D. Gesbert, "Predicting Device-to-Device Channels from Cellular Channel Measurements: A Learning Approach," *IEEE Trans. Wirel. Commun.*, vol. 19, no. 11, 2020.
- [40] Z. Becvar, D. Gesbert, P. Mach, and M. Najla, "Machine Learning-based Channel Quality Prediction in 6G Mobile Networks," *IEEE Communications Magazine*, vol. 61, no. 7, 2023.
- [41] Z. Becvar *et al.*, "Machine Learning for Channel Quality Prediction: From Concept to Experimental Validation," *IEEE Trans. Wirel. Commun.*, 2024.
- [42] H. Xiangwang *et al.*, "Distributed machine learning for autonomous agent swarm: A survey," *IEEE Commun. Surv. Tutor.*, 2025.
- [43] L. Mai *et al.*, "Applications of distributed machine learning for the internet-of-things: A comprehensive survey," *IEEE Commun. Surv. Tutor.*, vol. 27, no. 2, pp. 1053-1100, 2024.

- [44] P. Mach, Z. Becvar, and M. Najla, "Power allocation, channel reuse, and positioning of flying base stations with realistic backhaul," *IEEE Internet Things J.*, vol. 9, no. 3, pp. 1790-1805, 2021.
- [45] Y. Yin *et al.*, "Minimizing delay for MIMO-NOMA resource allocation in UAV-assisted caching networks," *IEEE Trans. Veh. Technol.*, vol. 72, no. 14, pp. 4728-4732, 2022.
- [46] M. Nikooroo, and Z. Becvar, "Optimization of total power consumed by flying base station serving mobile users," *IEEE Trans. Netw. Sci. Eng.*, vol. 9, no. 4, pp. 2815-2832, 2022.
- [47] Z. Hajiakhondi *et al.*, "Joint transmission scheme and coded content placement in cluster-centric UAV-aided cellular networks," *IEEE Internet Things J.*, vol. 9, no. 13, pp. 11098-11114, 2021.
- [48] A. Al-Hourani, S. Kandeepan, and S. Lardner, "Optimal LAP altitude for maximum coverage," *IEEE Wireless Commun. Lett.*, vol. 3, pp. 569-572, 2014.
- [49] J. Ji *et al.*, "Probabilistic cache placement in UAV-assisted networks with D2D connections: Performance analysis and trajectory optimization," *IEEE Trans. Commun.*, vol. 68, no. 10, pp. 6331-6345, 2020.
- [50] J. Yang, *et al.*, "Dynamic Convolution and Transformer Based Dual-Branch Coding in Semantic Communication System," *IEEE Communications Letters*, vol. 29, no. 5, pp. 161-1165, 2025.
- [51] R. Chai, *et al.*, "System Cost-Oriented UAV Deployment for Integrated Access and Backhaul Networks," *IEEE Trans. Veh. Technol.*, vol. 73, no. 9, pp. 12858-12872, 2024.
- [52] B. Simon, L. Wahl, and A. Klein, "A Socio-Technical Approach to Capacity Maximization for Device-to-Device Relay Selection," *IEEE ICC*, pp. 4671-4676, 2025.